Enhanced spin polarization of amorphous Fe_xSi_{1-x} thin films revealed by Andreev reflection spectroscopy

J. Karel,[1,2] D. S. Bouma,[2,3] J. Martinez,[4] Y. N. Zhang,[5] J. A. Gifford,[4] J. Zhang,[4] G. J. Zhao,[4] D. R. Kim,[4] B. C. Li,[4] Z. Y. Huang,[4] R. Q. Wu,[6] T. Y. Chen,[4,*] and F. Hellman[2,3]

[1]*Department of Materials Science and Engineering, Monash University, Clayton, VIC 3800, Australia*
[2]*Materials Sciences Division, Lawrence Berkeley National Lab, Berkeley, California 94720, USA*
[3]*Department of Physics, University of California Berkeley, Berkeley, California 94720, USA*
[4]*Department of Physics, Arizona State University, Tempe, Arizona 85287, USA*
[5]*School of Energy Science and Engineering, University of Electronic Science and Technology of China, Chengdu 611731, China*
[6]*Department of Physics and Astronomy, University of California, Irvine, California 92697, USA*

(Received 4 June 2017; published 27 June 2018)

Point contact Andreev reflection spectroscopy has been utilized to determine the spin polarization of both amorphous and crystalline Fe_xSi_{1-x} ($0.58 < x < 0.68$) thin films. The amorphous materials exhibited a substantial spin polarization (generally greater than 60%), despite significant changes in magnetization and resistivity. In particular, the polarization value in the $x = 0.65$ amorphous alloy is about 70%, significantly higher than most ferromagnets, including numerous Heusler compounds that are theoretically predicted to be half-metallic ferromagnets. The composition dependence of the spin polarization in the amorphous materials is proportional to (but substantially larger than) the DFT-calculated values. The polarization of a crystalline thin film with $x = 0.65$, by contrast, is only 49%, similar to that of common magnetic metals. The enhanced spin polarization in the amorphous structure is attributed to the modification of the local environments. This work demonstrates that the spin polarization, as well as magnetic moment, anomalous Hall effect, and electrical resistivity, can be tuned by introducing structural disorder as an engineering tool.

DOI: 10.1103/PhysRevMaterials.2.064411

Numerous spintronic applications, including magnetic tunnel junctions, spin-transfer torque magnetic random access memory, and spin injection into semiconductors, require materials with high spin polarization [1,2]. Heusler compounds have been investigated extensively for such applications. They present extremely tunable physical properties (e.g., magnetization, resistivity) that can be controlled with valence electron concentration, and many are predicted to be half-metallic ferromagnets, meaning full spin polarization at the Fermi energy [3]. Despite the theoretical half-metallic behavior, measurements of the spin polarization of Heusler compounds using point contact Andreev reflection (PCAR) have found values ranging from a maximum of 0.74 [$Co_2Mn(Ge_{0.75}Ga_{0.25})$] to as low as 0.48 ($Co_2VAl$) [4–6]. This reduction with respect to the theoretical value is typically understood as arising from chemical disorder, which in most cases degrades the spin polarization by introducing minority states in the gap [4,7–9]. A single notable measurement of spin-resolved ultraviolet photoemission spectroscopy on an $L2_1$-ordered Co_2MnSi epitaxial thin film grown and measured *in situ* demonstrated full half-metallicity (100% spin polarization), but in general, surface disorder, and possibly other effects such as surface segregation or contamination, reduce the spin polarization at the surface [10]. Such a situation is challenging for applications as chemical disorder is unlikely to be completely eliminated in thin film deposition at reasonable temperatures. Rather than attempting to minimize disorder, this work presents a different methodology—introducing complete structural disorder to *enhance* the spin polarization.

Fe_xSi_{1-x} ($0.45 < x < 0.75$) is an excellent system to demonstrate this approach since varying degrees of chemical and structural order are accessible using thin film growth [11,12]. The compositions of the films investigated in this work ($x = 0.58 - 0.68$), are near the so-called half-Heusler composition $x = 0.75$ with the chemically ordered $D0_3$ structure. The crystal structure unit cell has an fcc Bravais lattice and can be thought of as 8 bcc-like subunits with Fe (Fe_{II}) on the cube corners and Fe (Fe_I) and Si alternating in the body centers [13,14]. Partial ordering occurs in the off-stoichiometry ($x > 0.5$) $B2$ structure, where Fe is ordered at the cube corners (Fe_{II}), but Fe and Si randomly occupy the body center sites (Fe_I combined with Si sites). In the $A2$ structure, there is no long-range chemical ordering, but bcc structural order is maintained. Finally, amorphous thin films can also be fabricated. Previous work has shown that the amorphous materials exhibit an enhanced magnetic moment [Fig. 1(a)] and large anomalous Hall effect [15,16]; both are related to the local atomic environment. In the former, the large magnetic moment is due to the reduction in the number of Fe-Si bonds which reduces *p-d* hybridization. In the latter, the large AHE likely originates from the topology of the local electronic structure, which in a system possessing long range order is typically expressed as a momentum-space integral of the Berry phase but in a system lacking long-range order has an equally valid real-space formulation, constructed in Ref. [17], which

*tingyong.chen@asu.edu

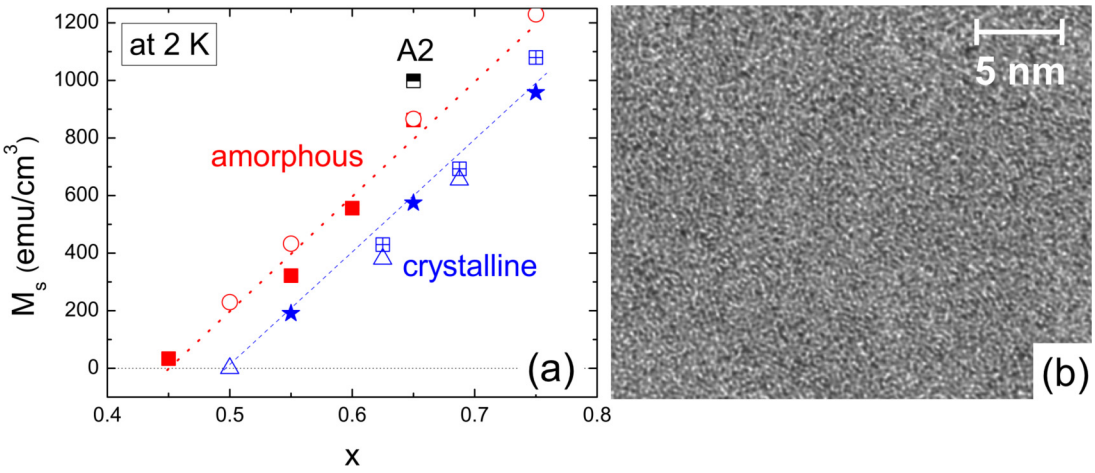

FIG. 1. (a) Saturation magnetization at 2 K versus x for amorphous and crystalline Fe_xSi_{1-x}. The open symbols are theoretical calculations, and the closed symbols are experimental data points. The blue open triangles (blue boxes with cross) are theoretical values for the $B2$ ($D0_3$) structure (note that $B2$ and $D0_3$ have nearly the same M as each other), with solid stars showing the experimental values. The black square divided horizontally is the theoretical result for the $A2$ structure (also labeled directly); this structure has no experimental value, as it was never successfully fabricated. All experimental data points were measured at 2 K. Further details of the theoretical calculations can be found in Ref. [15]. (b) Cross section HRTEM on a representative $x = 0.55$ amorphous sample.

corroborates our finding that the AHE is associated with local order.

In this work we show that the spin polarization remains high (>60%) in the amorphous thin films, even with reduced Fe content. We further compare amorphous and epitaxial films with $x = 0.65$ and find that remarkably, the spin polarization is significantly larger in the disordered amorphous material. The spin polarization in this amorphous thin film is very near the largest reported value using PCAR for any Heusler material [$Co_2Mn(Ge_{0.75}Ga_{0.25})$] and is larger than PCAR measurements on Heusler compounds that are theoretically predicted to be half-metallic (e.g., Co_2FeSi,Co_2FeAl) [6].

The spin polarization (P) of a metal is defined as the normalized imbalance of the density of states (DOS) of the two spin orientations at the Fermi level $P \equiv [N(E_{F\uparrow}) - N(E_{F\downarrow})]/[N(E_{F\uparrow}) + N(E_{F\downarrow})]$, with $N(E_{F\uparrow})$ and $N(E_{F\downarrow})$, respectively, as the spin-up and spin-down DOS. Point contact Andreev reflection (PCAR) is one of the few methods that can determine the P value of magnetic materials; other methods include tunneling magnetoresistance (where P can be extracted using Julliere's model) and spin-resolved photoemission [10,18]. At a normal metal/superconductor (S) interface, when an electron is injected into S, it must be accompanied by another electron with opposite spin to enter together as a Cooper pair, causing a hole to be reflected back into the normal metal. This is the Andreev reflection [19]. Because of Andreev reflection, for a normal metal with $P = 0$, the conductance within the superconducting gap (Δ) is twice that outside the gap because each electron can carry another electron to form a Cooper pair. For a half metal ($P = 1$), there is only one spin band at the Fermi level, hence the conductance within the gap is zero because the required Cooper pair cannot be formed. For most magnetic metals, the P value is between 0 and 1, a linear combination of the two cases. These are the expected situations for an ideal interface at zero temperature ($T = 0$). In reality, there is often interfacial scattering Z, inelastic scattering Γ, and extra resistance (r_E) [20]. The P value is extracted using a modified Blonder-Tinkham-Klapwijk (BTK) model [20–23] to fit the data with all of these effects incorporated.

Amorphous Fe_xSi_{1-x} thin films of 120–150 nm were grown by electron beam co-evaporation of Fe and Si at room temperature on an amorphous SiN_x on Si substrate. The epitaxial $Fe_{0.65}Si_{0.35}$ film of similar thickness was fabricated by growing at room temperature on a Cr buffer layer that was deposited on (001) MgO at 200 °C. The amorphous and crystalline nature has been confirmed by x-ray diffraction and high-resolution transmission electron microscopy [Fig. 1(b)]. The magnetic, structural, and growth details of the samples probed here have been described elsewhere [11,12,15]. A thin Al capping layer of 1.5 nm is deposited on all samples to protect the surface from oxidation for the spin polarization experiments. In this work we determine the spin polarization of the amorphous and crystalline Fe_xSi_{1-x} alloys using PCAR. A superconducting tip of a few nm in size is used in the experiments. The sample and the tip are enclosed in a vacuum jacket that is cooled to temperatures between 1.65 and 4.2 K. A point contact is then established and the differential conductance dI/dV and resistance V/I were measured using a lock-in method. With a slightly different pressure, a new contact is achieved, which often has a different contact resistance and a different interfacial scattering factor Z discussed below. Both superconducting Nb and Pb tips have been utilized and there is no observable difference in the determined P values. The resistivity of the epitaxial sample is 54 $\mu\Omega$ cm while it is between 200–500 $\mu\Omega$ cm for the amorphous samples, depending on x [16]. In our experiments, the contact resistance (R_C) is between 71 and 300 Ω where the corresponding contact size is a few nm, less than or comparable to the mean free path estimated from the resistivity based on the Drude model in the crystalline sample. For the amorphous sample, contacts are close to the diffusive regime, an important consideration in fitting the extra resistance that is described below.

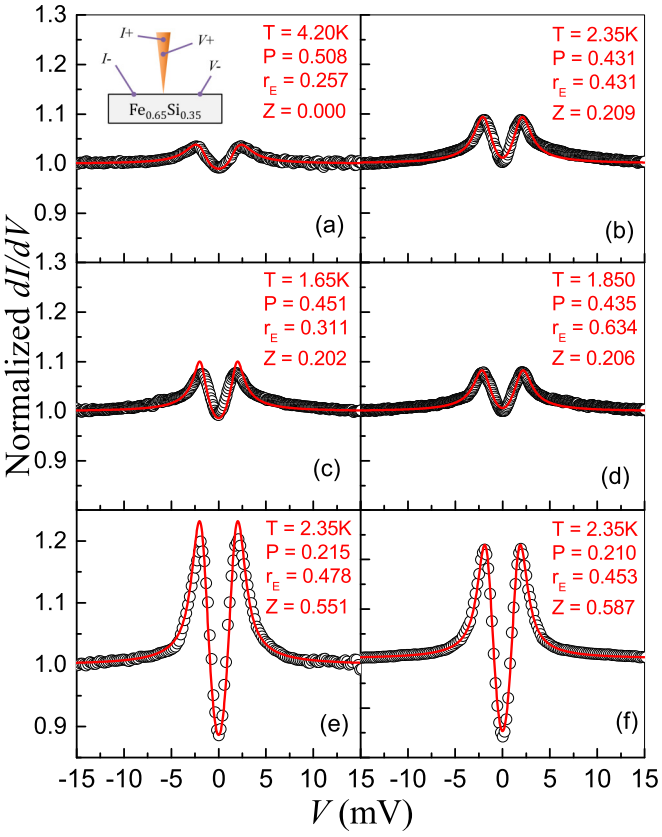

FIG. 2. (a)–(f) Representative Andreev spectra (open circles) of different Z factor from 0 to 0.59 of Pb point contacts on an epitaxial $Fe_{0.65}Si_{0.35}$ sample and the best fits to the modified BTK model (solid curves) with the superconducting gap of Pb $\Delta \approx 1.30$ meV, Z the interfacial scattering factor, and r_E the additional resistance. Inset is the schematic setup of a point contact.

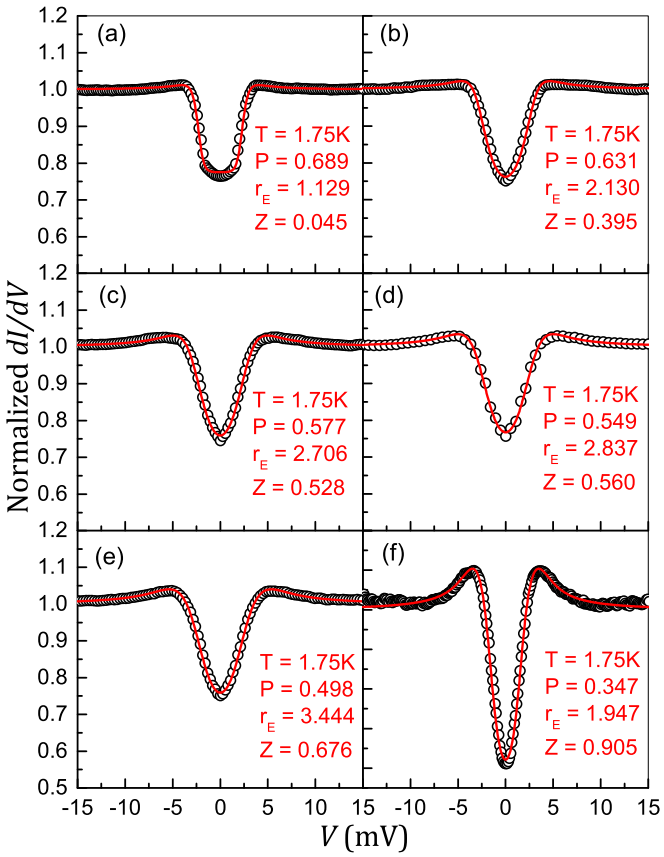

FIG. 3. Representative Andreev spectra (open circles) of different Z factor from 0.05 to 0.91 of point contacts on an amorphous $Fe_{0.65}Si_{0.35}$ sample and the best fits to the modified BTK (solid curves).

The schematic setup of a point contact is illustrated by the inset in Fig. 2(a) where two electrodes are separately attached to the tip and the sample. Some representative PCAR spectra are shown in Fig. 2 for Pb tips in contact with the crystalline $x = 0.65$ sample. The open circles are the experimental data while the solid curves are the best fit using the modified BTK model. The fitting parameters are listed inside each panel. The data are well described by the model. As Z increases, the P value of the epitaxial $Fe_{0.65}Si_{0.35}$ sample decreases from about 50% at $Z = 0$ to 20% at $Z = 0.6$, showing a typical reduction of the P value by the interfacial scattering (some of which is spin flip) that is also observed in other ferromagnets [24–26]. The intrinsic value of P is obtained by extrapolation of the measured P values to $Z = 0$. The superconducting gap Δ value is often indicated by the two Andreev shoulder peaks, but in our data the two Andreev peaks are at about ± 2.5 mV, much larger than the experimental value $\Delta(0) = 1.34$ meV of the Pb tip calculated from the T_C using the BCS theory. This increase is due to the extra resistance resulting from the relatively high resistivity of the sample. The effect of the extra resistance can be taken into account in PCAR by introducing a dimensionless factor r_E, which is defined as the resistance of the sample in series with the contact resistance (R_C), normalized by R_C. The resistance contribution from the sample depends on the size of the contact [20], so r_E can only be obtained via analysis of the experimental PCAR spectra. The effect of r_E on the PCAR spectra has been previously described in detail [20]. In our analysis, the temperature and the superconducting gap are fixed as experimental values while only r_E, P, and the Z factor are varied. In fact, even with all the parameters free, the resultant T and Δ are very similar to these fixed experimental values, demonstrating that it is possible (and important) to take the additional resistance into account for data analysis in these samples with higher resistivity. The Γ factor, often accounting for the quality of the superconductor tip, is found to be negligible when it is allowed to vary in the fit, and was therefore set to 0 to limit the number of variables in the fits.

Next, we consider the P value of the amorphous samples, also measured using Pb tips. Some representative spectra are shown in Fig. 3 ($x = 0.65$) and Fig. 4 ($x = 0.58, 0.62$, and 0.68) where open circles are experimental data and solid curves are the best fit to the modified BTK model. Obviously, as shown in Figs. 3 and 4, PCAR spectra of the amorphous samples are very different from that of the crystalline sample. The dip near zero bias voltage is much lower than that of the spectra of the crystalline sample, indicating a higher P value. Indeed, the P value for the $x = 0.65$ sample obtained using the BTK model is significantly higher, 68.9% at $Z = 0.045$, as shown in Fig. 3(a). The P value of the amorphous samples decreases for increasing Z, showing a similar trend as that of the crystalline sample. One also notes that the Andreev peaks now appear close to ± 5 mV, much larger than the Δ value of the Pb tip,

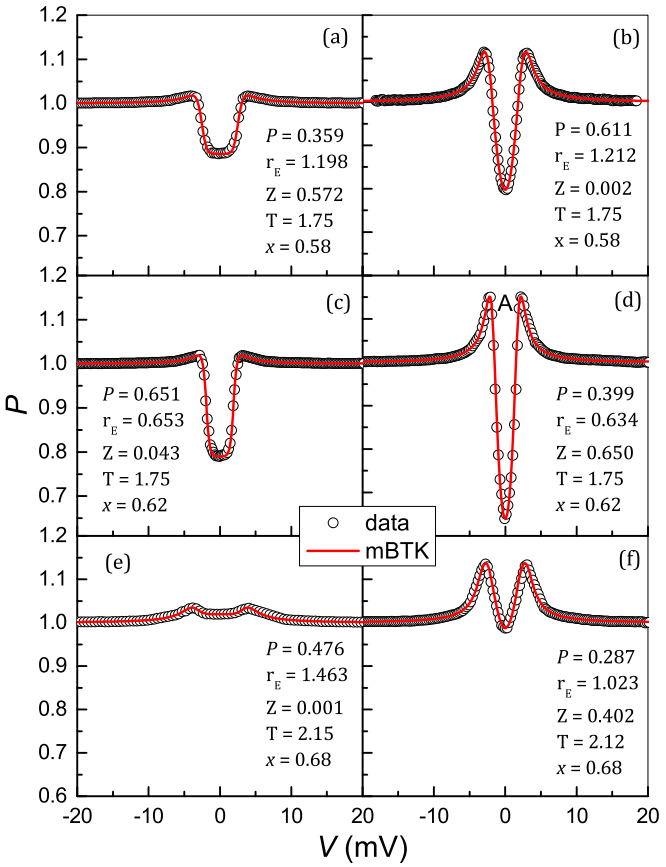

FIG. 4. Representative Andreev spectra (open circles) of amorphous Fe_xSi_{1-x}. (a) and (b) For $x = 0.58$, (c) and (d) for $x = 0.62$, and (e) and (f) for $x = 0.68$ where open circles are experimental data and solid curves are the best fits to the modified BTK with parameter inset.

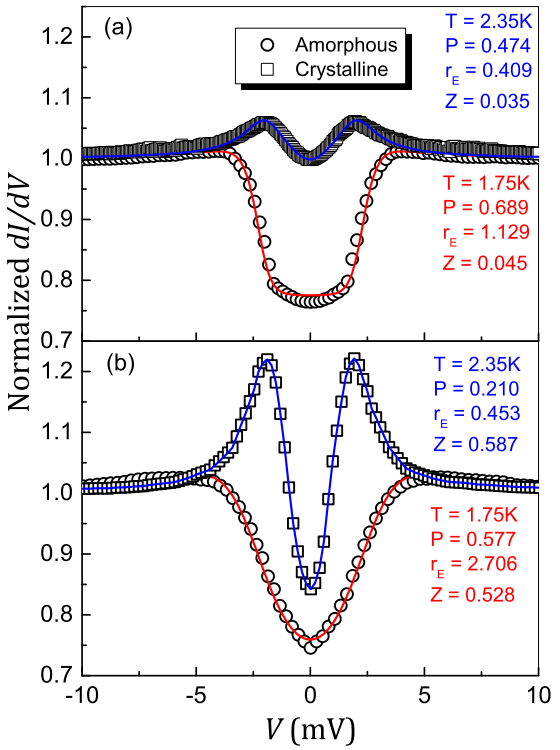

FIG. 5. Comparison of Andreev spectra of two contacts on the amorphous and the epitaxial $Fe_{0.65}Si_{0.35}$ samples with (a) small Z factor close to zero and (b) large Z factor of about 0.5 where open symbols are the experimental data and the solid curves are the best fit to the BTK model.

due to the extra resistance r_E; the obtained r_E values are indeed much larger than in the epitaxial sample, consistent with the high resistivity of the amorphous sample.

PCAR determines the P value based on the suppression of the Andreev reflection by a spin polarized current. The higher the P value, the lower the entire PCAR spectrum is. On the other hand, the interfacial scattering factor Z causes a dip at zero bias with two shoulder peaks. The larger the Z factor, the lower the dip and the higher the two shoulder peaks. Therefore, it is important to compare the PCAR spectra with similar Z factors to reveal the difference in spin polarization. As shown in Fig. 5, two spectra with very different Z values ($Z \approx 0$ and $Z > 0.5$ from the $x = 0.65$ crystalline sample are compared, respectively, to those of the $x = 0.65$ amorphous sample. The normalized conductance (black squares) for the crystalline sample is about 1.05 at zero bias for $Z = 0.035$, while the conductance (black circles) for the amorphous sample is only 0.75, indicating a much higher P value of the amorphous sample. Even for large $Z > 0.5$, the whole conductance spectrum of the crystalline sample is still much higher than that of the amorphous sample, as shown in Fig. 5(b).

Over 40 PCAR spectra were measured for each sample, and the obtained P values are plotted in Fig. 6, where the open symbols are the P values obtained using the modified BTK model. The Z factors for the amorphous samples are larger than those obtained from the crystalline sample. This result is most likely due to the reduced mean free path of the amorphous sample [16], which causes the contact to be closer to the diffusive regime. In this regime, the P value can still be determined by considering a slightly higher Z factor [20]. The P value decreases for increasing Z factor for both amorphous and crystalline samples, but at any Z factor, the P value of the amorphous sample is higher than that of the crystalline sample (except $x = 0.68$ amorphous, which is roughly the same as the crystalline $x = 0.65$ sample). Extrapolating the Z factor to zero, we obtain the intrinsic P value. For the crystalline $Fe_{0.65}Si_{0.35}$ sample, the P value is $49.0 \pm 0.4\%$, close to the previously reported value in epitaxial Fe_3Si of $45 \pm 5\%$ [27]. However, the P value for the amorphous $Fe_{0.65}Si_{0.35}$ sample is $70.0 \pm 1.3\%$, significantly higher than that of the crystalline sample. A summary of the spin polarizations from this work and other previous work, including both theory and experiment, is given in Table I for Fe_xSi_{1-x} with different x and chemical order, as indicated.

The DOS (and therefore the P value) in a crystalline solid result from the energy bands $E(\mathbf{k})$, which are governed by the periodicity and symmetry of the lattice. Band dispersion curves $E(\mathbf{k})$ are not well defined in amorphous materials, which only possess short-range order. Nevertheless, there is still a well-defined Fermi energy E_F and density of electronic states, and the conduction electrons in an amorphous ferromagnetic metal should remain polarized. Indeed, an enhanced P value has been reported in amorphous CoFeB (0.65 versus 0.53 in partially crystalline CoFeB) [25]. The work presented here

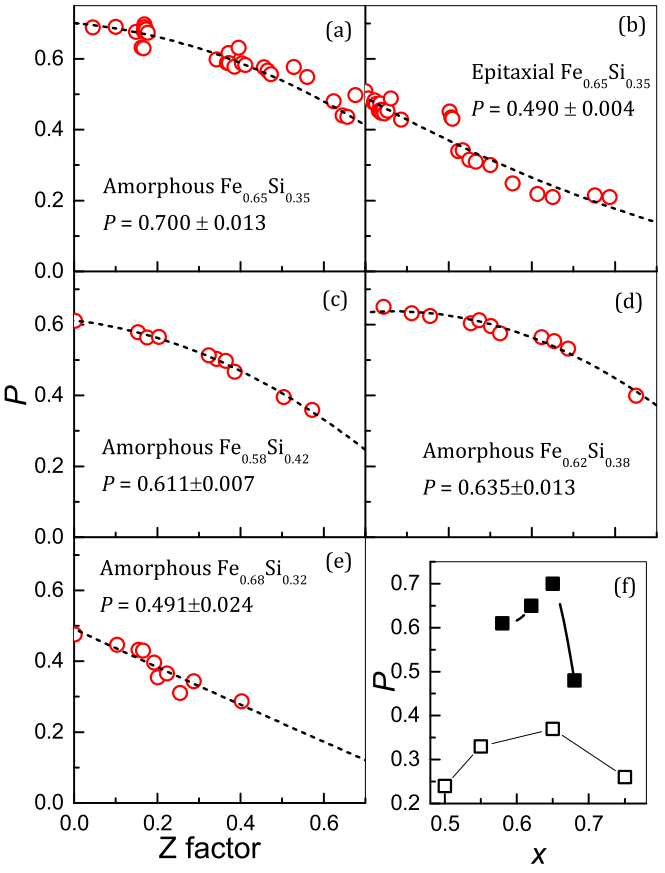

FIG. 6. Spin polarization from different point contacts of the amorphous (a) and epitaxial (b) $Fe_{0.65}Si_{0.35}$ samples, and for amorphous $Fe_{0.58}Si_{0.42}$ (c), $Fe_{0.62}Si_{0.38}$ (d), and $Fe_{0.68}Si_{0.32}$ (e) as a function of Z factor (dashed lines are quadratic fits to guide the eye.). (f) Spin polarization of amorphous Fe_xSi_{1-x} as a function of x. The filled squares are experimental data, and the open squares are theoretical calculations.

shows that the P value of the amorphous $Fe_{0.65}Si_{0.35}$ thin film is also substantially higher (0.7 versus 0.49) than that of the crystalline alloy with the same composition. Other compositions also exhibit considerable spin polarization, greater than 0.6 (except for $x = 0.68$). As previously mentioned, the magnetism in the Fe_xSi_{1-x} system is actually enhanced in the amorphous materials due to the reduction in the number of Fe-Si bonds, which reduces *p-d* hybridization (see Fig. 1(a) and Ref. [15]). Similar to the enhanced magnetic moment, the large spin polarization likely originates from the modifications in the local atomic environments produced in the amorphous structure. It is well known that in amorphous transition metal-Si (or Ge) materials, Si (or Ge) tries to maintain a tetrahedral bond environment, even in the absence of long-range order [28–32]. This fact and our present results suggest there may be other amorphous transition metal-Si (or Ge) compounds which present similar enhancements in magnetization and spin polarization.

We now turn to a comparison of the experimental spin polarization and previous theoretical predictions from density functional theory (DFT), which are both found in Table I. Considering theory and experiment for a given x and order,

TABLE I. Summary of experimental and theoretical spin polarizations for different order and x in Fe_xSi_{1-x}. The experimental and theoretical values for the $x = 0.75$ $D0_3$ material are from Refs. [27,33], respectively. All details for the other theoretically calculated spin polarizations can be found in Refs. [11,15]. Note that the DOS and spin polarization for the $x \sim 0.65$ $D0_3$ and $B2$ compositions are calculated using a supercell structure, meaning only certain stoichiometries can be accessed due to the total number of atoms in the supercell. The exact composition is $x = 0.63$; thus $x \sim 0.65$ is used in the table. Note that PCAR is not sensitive to the spin polarization sign; in this table, the absolute values are shown and additional experiments would be required to determine the sign of P.

Composition	Order	Experimental $\lvert P\rvert$ (PCAR)	Theoretical P
$x = 0.75$	$D0_3$	0.45	0.30
$x = 0.75$	Amorphous		−0.26
$x = 0.68$	Amorphous	0.49	
$x \sim 0.65$	$D0_3$		0.76
$x \sim 0.65$	$B2$	0.49	0.48
$x = 0.65$	$A2$		−0.12
$x = 0.65$	Amorphous	0.70	−0.37
$x = 0.62$	Amorphous	0.64	
$x = 0.58$	Amorphous	0.61	
$x = 0.55$	Amorphous		−0.33
$x = 0.50$	Amorphous		−0.24

the spin polarization of the $B2$ structure is similar. For $D0_3$, at $x = 0.75$, theory and experiment are both relatively low; the origin of the difference between experiment and theory for $x = 0.75$ $D0_3$ is not clear, although the authors reported the possibility of chemical disorder and slight variations in stoichiometry [27,33]. For the off-stoichiometric $x = 0.65$ $D0_3$ structure, the *theoretical* P is quite large, an as-yet untested prediction. Finally, the experimental values of the spin polarization for the amorphous compositions are substantially larger than the theoretical values, although the composition dependence is qualitatively remarkably similar (i.e., the spin polarization increases up to $x = 0.65$, then decreases), as can also be seen in Fig. 6(f). The difference between experiment and theory for the amorphous structure may be related to the small size of the supercell used in the calculations.

In summary, we have determined the spin polarization of both amorphous and epitaxial Fe_xSi_{1-x} ($0.58 < x < 0.68$) thin films. Amorphous thin films with a range of Fe concentrations (from $x = 0.58$ to $x = 0.65$) exhibited spin polarizations greater than 60%, despite significant variations in magnetization and resistivity. We compared directly the spin polarization measured in amorphous and crystalline thin films with $x = 0.65$. The spin polarization of the epitaxial sample in this comparison is about 49%, similar to that of common magnetic metals, indicating that it is a good spin injector for semiconductor spintronics. Remarkably, the spin polarization of the amorphous $Fe_{0.65}Si_{0.35}$ alloy is about 70%, which is substantially higher than PCAR experimental values reported in Heusler compounds that are theoretically half-metallic (∼60%) and even approaches the highest reported spin polarization measured by PCAR in a Heusler compound (74%). This work ultimately suggests structural disorder might

be harnessed as an engineering tool to enhance the magnetic properties in transition metal alloys. Moreover, the opportunity to enhance the magnetic moment, anomalous Hall effect, and spin polarization with deposition at room temperature (and no subsequent annealing) is extremely attractive for integration into spintronic devices. We hope these results will stimulate further investigations in amorphous materials generally, and these Fe-Si alloys specifically.

This work was primarily supported by the U.S. Department of Energy, Office of Science, Basic Energy Sciences, Materials Sciences and Engineering Division under Contract No. DE-AC02-05-CH11231 within the non-equilibrium magnetic materials (NEMM) program (MSMAG). Andreev reflection measurements were supported as part of SHINES, an Energy Frontier Research Center funded by the U.S. Department of Energy, Office of Science under Award SC0012670. DFT calculations at UCI were supported by DOE-BES (Grant No. DE-FG0205ER46237) and the computer simulations were supported by the National Energy Research Scientific Computing Center (NERSC). The authors thank David Smith for cross-section HRTEM measurements.

[1] I. Zutic, J. Fabian, and S. D. Sarma, Rev. Mod. Phys. **76**, 323 (2004).
[2] D. C. Ralph and M. D. Stiles, J. Magn. Magn. Mater. **320**, 1190 (2008).
[3] T. Graf, C. Felser, and S. S. P. Parkin, Prog. Solid State Chem. **39**, 1 (2011).
[4] Y. K. Takahashi, A. Srinivasan, B. Varaprasad, A. Rajanikanth, N. Hase, T. M. Nakatani, S. Kasai, T. Furubayashi, and K. Hono, Appl. Phys. Lett. **98**, 152501 (2011).
[5] S. V. Karthik, A. Rajanikanth, Y. K. Takahashi, T. Ohkubo, and K. Hono, Acta Mater. **55**, 3867 (2007).
[6] B. S. D. Ch. S. Varaprasad, A. Srinivasan, Y. K. Takahashi, M. Hayashi, A. Rajanikanth, and K. Hono, Acta Mater. **60**, 6257 (2012).
[7] S. V. Karthik, A. Rajanikanth, Y. K. Takahashi, T. Okhubon, and K. Hono, Appl. Phys. Lett. **89**, 052505 (2006).
[8] T. M. Nakatani, A. Rajanikanth, Z. Gercsi, Y. K. Takahashi, K. Inomata, and K. Hono, J. Appl. Phys. **102**, 033916 (2007).
[9] B. S. D. Ch. S. Varaprasad, A. Rajanikanth, Y. K. Takahashi, and K. Hono, Appl. Phys. Express **3**, 023002 (2010).
[10] M. Jourdan, J. Minar, J. Braun, A. Kronenberg, S. Chadov, B. Balke, A. Gloskovskii, M. Kolbe, H. J. Elmers, G. Schonhense, H. Ebert, C. Felser, and M. Klaui, Nat. Commun. **5**, 3974 (2014).
[11] J. Karel, J. Juraszek, J. Minar, C. Bordel, K. H. Stone, Y. N. Zhang, J. Hu, R. Q. Wu, H. Ebert, J. B. Kortright, and F. Hellman, Phys. Rev. B **91**, 144402 (2015).
[12] A. X. Gray, J. Karel, J. Minár, C. Bordel, H. Ebert, J. Braun, S. Ueda, Y. Yamashita, L. Ouyang, D. J. Smith, K. Kobayashi, F. Hellman, and C. S. Fadley, Phys. Rev. B **83**, 195112 (2011).
[13] D. Berling, G. Gewinner, M. C. Hanf, K. Hricovini, S. Hong, B. Loegel, A. Mehdaoui, C. Pirri, M. H. Tuilier, and P. Wetzel, J. Magn. Magn. Mater. **191**, 331 (1999).
[14] W. A. Hines, A. H. Menotti, J. I. Budnick, T. J. Burch, T. Litrenta, V. Niculescu, and K. Raj, Phys. Rev. B **13**, 4060 (1976).
[15] J. Karel, Y. N. Zhang, C. Bordel, K. H. Stone, T. Y. Chen, C. A. Jenkins, D. J. Smith, J. Hu, R. Q. Wu, S. M. Heald, J. B. Kortright and F. Hellman, Mater. Res. Express **1**, 026102 (2014).
[16] J. Karel, C. Bordel, D. S. Bouma, A. de Lorimier-Farmer, H. J. Lee, and F. Hellman, Europhys. Lett. **114**, 57004 (2016).
[17] A. Marrazzo and R. Resta, Phys. Rev. B **95**, 121114(R) (2017).
[18] M. Julliere, Phys. Lett. A **54**, 225 (1975).
[19] A. F. Andreev, Sov. Phys. JETP **19**, 1228 (1964).
[20] T. Y. Chen, S. X. Huang, and C. L. Chien, Phys. Rev. B **81**, 214444 (2010).
[21] G. T. Woods, R. J. Soulen, Jr., I. I. Mazin, B. Nadgorny, M. S. Osofsky, J. Sanders, H. Srikanth, W. F. Egelhoff, and R. Datla, Phys. Rev. B **70**, 054416 (2004).
[22] P. Chalsani, S. K. Upadhyay, O. Ozatay, and R. A. Buhrman, Phys. Rev. B **75**, 094417 (2007).
[23] T. Y. Chen, Z. Tesanovic, and C. L. Chien, Phys. Rev. Lett. **109**, 146602 (2012).
[24] T. Y. Chen, C. L. Chien, and C. Petrovic, Appl. Phys. Lett. **91**, 142505 (2007).
[25] S. X. Huang, T. Y. Chen, and C. L. Chien, Appl. Phys. Lett. **92**, 242509 (2008).
[26] J. S. Parker, S. M. Watts, P. G. Ivanov, and P. Xiong, Phys. Rev. Lett. **88**, 196601 (2002).
[27] A. Ionescu, C. A. F. Vaz, T. Trypiniotis, C. M. Gürtler, H. García-Miquel, J. A. C. Bland, M. E. Vickers, R. M. Dalgliesh, S. Langridge, Y. Bugoslavsky, Y. Miyoshi, L. F. Cohen, and K. R. A. Ziebeck, Phys. Rev. B **71**, 094401 (2005).
[28] L. Zeng, J. X. Cao, E. Helgren, J. Karel, E. Arenholz, L. Ouyang, D. J. Smith, R. Q. Wu, and F. Hellman, Phys. Rev. B **82**, 165202 (2010).
[29] W. A. Phillips, J. Low Temp. Phys. **7**, 351 (1972).
[30] D. R. Queen, X. Liu, J. Karel, T. H. Metcalf, and F. Hellman, Phys. Rev. Lett. **110**, 135901 (2013).
[31] X. Liu, D. R. Queen, T. H. Metcalf, J. E. Karel, and F. Hellman, Phys. Rev. Lett. **113**, 025503 (2014).
[32] D. R. Queen, X. Liu, J. Karel, H. C. Jacks, T. H. Metcalf, and F. Hellman, J. Non-Cryst. Solids **426**, 19 (2015).
[33] M. Lezaic, P. Mavropoulos, S. Blugel, and H. Ebert, Phys. Rev. B **83**, 094434 (2011).